An Invariant Measure of Disorder in Patterns

Gemunu H. Gunaratne* and Ronald E. Jones†
Department of Physics, The University of Houston, Houston, Texas 77204

Qi Ouyang‡ and Harry L. Swinney§
Center for Nonlinear Dynamics and Department of Physics, The University of Texas at Austin, Austin, Texas 78712
(Received 3 May 1995)

An invariant measure is introduced to quantify the disorder in extended locally striped patterns. The measure is invariant under Euclidean motions of the pattern, and vanishes for a uniform array of stripes. Irregularities such as point defects and domain walls make nonzero contributions to the measure. Analysis of patterns generated in a reaction-diffusion system suggests two additional properties of the measure: (1) Apart from small fluctuations, it is invariant for distinct patterns generated at fixed control parameters. (2) It exhibits a jump at the onset of pattern dynamics.

PACS numbers: 47.54.+r, 47.20.Hw, 47.20.Ky, 82.40.Bj

Spatiotemporal dynamics govern the evolution of most physical and biological systems, e.g., weather patterns, earthquake dynamics, and cardiac rhythms. Comparison of different disordered patterns in such complex systems is hampered by the absence of suitable global variables to quantify the disorder. Global invariants, such as generalized dimensions and expansion rates, have proven useful in the quantitative analysis of low dimensional chaotic systems [1]. However, attempts to use fractal dimensions and Lyapunov exponents to quantify spatiotemporal dynamics from time signals have not been successful. Moreover, these measures do not capture the essential spatial characteristics of a pattern. In this Letter we introduce an invariant measure, the *disorder parameter* δ_1, which quantifies the "amount of disorder" in an extended pattern. An analysis of experimental patterns suggests that it is invariant (apart from statistical fluctuations) for distinct patterns generated at fixed control parameters. Rather remarkably, this purely static measure undergoes a sharp increase near the onset of time dependence in the spatial patterns.

We analyze patterns that have been obtained in a laboratory study of a chlorite-iodide-malonic acid reaction in a spatially extended open reactor [2]. The patterns form in a thin disk of polyacrylamide gel, which is sandwiched between two thin porous glass disks that are in contact with continuously fed well-stirred reservoirs; the reagents in each reservoir are nonreacting [3]. The gel prevents convection but allows for the diffusion of chemicals; the homogeneous, temperature-controlled reservoirs provide well-defined boundary conditions for the reaction-diffusion system. Beyond critical values of the control parameters (i.e., reagent concentrations, flow rate of reagents into the reservoirs, gel thickness, and reactor temperature), patches of regular spatial patterns (hexagons or stripes) spontaneously emerge from a spatially uniform background [4]. The wavelength of the patterns is fairly constant over the whole system. The pattern evolves into a large mosaic of domains with different orientations, as Figs. 1(a) and 1(b) illustrates. If the system is driven further from the onset of instability (e.g., by changing the malonic acid concentration gradient between the two reservoirs), a critical control parameter value is reached at which the pattern becomes time dependent [2]. A close comparison between stationary patterns [e.g., Figs. 1(a) and 1(b)] and moving patterns [e.g., Figs. 1(c)–1(f)] reveals different amounts of disorder. The stationary patterns have larger domains of stripes of a single orientation, while the moving patterns have more domain walls and defects. The parameter δ_1 quantifies the observed variation of disorder and permits a comparison between the amount of disorder in distinct patterns. We consider here patterns that consist of local patches of stripes, but the extension of our results to other systems and to patterns consisting of local patches of other planforms is conceptually straightforward.

The disorder in the pattern is measured with respect to stripes of a given size; $\delta_1 = 0$ for a perfect array of stripes. Any reasonable measure of the disorder should be invariant under translations, reflections, and rotations of the extended pattern (e.g., moving or rotating the entire pattern should not change the value of the disorder parameter). In addition, if the measure of disorder is to be useful in characterizing real (noisy) laboratory data, it should require only low order derivatives of the characterizing field $U(\mathbf{x})$ (which for the reaction-diffusion system, is the relative concentration of a product). The disorder parameter defined below satisfies each of these conditions.

Since the pattern is locally striped, the field $U(\mathbf{x})$ can be expanded as

$$U(\mathbf{x}) = A(\mathbf{x})e^{i\mathbf{k}\cdot\mathbf{x}} + \text{c.c.}, \tag{1}$$

where the complex field $A(\mathbf{x})$ is the *envelope function* [5]. The magnitude of $\mathbf{k}$ is $k_0 = 2\pi/\lambda$, λ being the characteristic wavelength of the pattern. The addition of the complex conjugate c.c. allows the field $U(\mathbf{x})$ to be real. Since the basic state $e^{i\mathbf{k}\cdot\mathbf{x}}$ is factored out of $U(\mathbf{x})$, the envelope function varies on a scale large compared

0031-9007/95/75(18)/3281(4)$06.00

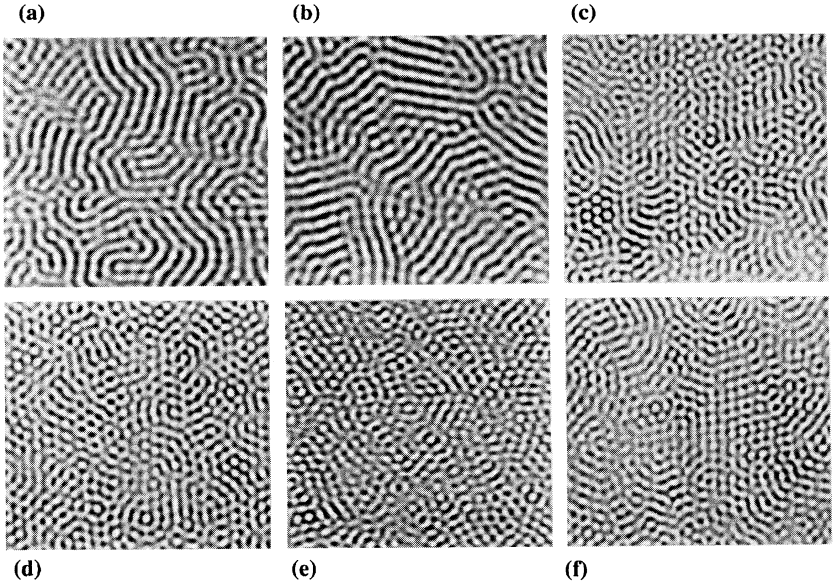

FIG. 1. Patterns generated in a reaction-diffusion system involving a chlorite-iodide-malonic acid reaction in a thin disk reactor. The reaction occurs in a thin layer of polyacrylamide gel sandwiched between two reservoirs, A and B. The malonic acid concentrations in reservoir B were (a) 12.0, (b) 11.0, (c) 10.0, (d) 9.0, (e) 8.0, and (f) 7.0 mM; the malonic acid concentration in reservoir A was 0. Other control parameters were held fixed at $[I^-]_0^{A,B} = 3.0$ mM, $[Na_2SO_4]_0^{A,B} = 4.5$ mM, $[ClO_2^-]_0^A = 18$ mM, $[ClO_2^-]_0^B = 0$ mM, $[H_2SO_4]_0^A = 0.5$ mM, $[H_2SO_4]_0^B = 20$ mM, temperature 7.0 °C, and gel thickness 2.0 mm. The transition from stationary to time-dependent patterns occurs at a concentration 10.5 mM of malonic acid in reservoir B.

with λ. Consequently, the expansion (1) can also be used to reduce the experimental noise, through suitable local averaging.

The disorder parameter is defined in terms of the envelope function $A(\mathbf{x})$ as

$$\delta_1 = \frac{1}{k_0^2 \langle |A(\mathbf{x})| \rangle} \int\int |\odot A(\mathbf{x})|\, dx\, dy\,, \tag{2}$$

where $\langle |A(\mathbf{x})| \rangle$ is the mean value of $|A(\mathbf{x})|$ over the pattern and the operator $\odot \equiv \odot(\partial_x, \partial_y)$ is defined by [6,7]

$$\odot = \mathbf{k} \cdot \nabla - (i/2)\nabla^2. \tag{3}$$

The domain of integration is the area of the pattern. δ_1 is normalized so that the disorder per unit area $\bar{\delta}_1 \equiv \delta_1 / \int\int dx\, dy)$ is dimensionless, and hence scale invariant.

We first show that δ_1 vanishes for an extended array of stripes pointing normal to an *arbitrary* direction $\mathbf{k}'$, with $|\mathbf{k}'| = k_0$. The field $U'(\mathbf{x})$ for this array can be expanded as $U'(\mathbf{x}) = A'(\mathbf{x}) e^{i\mathbf{k}\cdot\mathbf{x}}$ with $A'(\mathbf{x}) = a e^{i(\mathbf{k}'-\mathbf{k})\cdot\mathbf{x}}$, with a being the (constant) amplitude. Now

$$\begin{aligned} \odot A'(\mathbf{x}) &= iA'(\mathbf{x})[\mathbf{k} \cdot (\mathbf{k}' - \mathbf{k}) + \tfrac{1}{2}(\mathbf{k}' - \mathbf{k})^2] \\ &= \tfrac{1}{2} iA'(\mathbf{x})\,(\mathbf{k}'^2 - \mathbf{k}^2) = 0\,, \end{aligned} \tag{4}$$

the last equality following from $|\mathbf{k}'| = |\mathbf{k}| = k_0$.

Next we show that the disorder parameter of an extended pattern is invariant under rotations of the pattern, or equivalently that δ_1 for a given field $U(\mathbf{x})$ is independent of the direction $\mathbf{k}$ chosen for the expansion (1). If the expansion about a second vector $\mathbf{k}'$ is written as $U(\mathbf{x}) = A'(\mathbf{x}) e^{i\mathbf{k}'\cdot\mathbf{x}}$ + c.c., then $A'(\mathbf{x}) = A(\mathbf{x}) e^{i(\mathbf{k}-\mathbf{k}')\cdot\mathbf{x}}$. Writing $\odot' = \mathbf{k}' \cdot \nabla - (i/2)\nabla^2$, we have

$$\begin{aligned} \odot' A'(\mathbf{x}) &= [\mathbf{k}' \cdot \nabla - (i/2)\nabla^2] A(\mathbf{x}) e^{i(\mathbf{k}-\mathbf{k}')\cdot\mathbf{x}} \\ &= e^{i(\mathbf{k}-\mathbf{k}')\cdot\mathbf{x}} \{(\mathbf{k}' \cdot \nabla)A(\mathbf{x}) + i\mathbf{k}' \cdot (\mathbf{k} - \mathbf{k}')A(\mathbf{x}) - (i/2)[\nabla^2 A(\mathbf{x}) - (\mathbf{k} - \mathbf{k}')^2 A(\mathbf{x})] + [(\mathbf{k} - \mathbf{k}') \cdot \nabla] A(\mathbf{x})\} \\ &= e^{i(\mathbf{k}-\mathbf{k}')\cdot\mathbf{x}} \odot A(\mathbf{x})\,. \end{aligned} \tag{5}$$

It follows that δ_1 is independent of the direction of expansion $\mathbf{k}$, as we needed to show. The invariance of δ_1 under translations and reflections follows from similar calculations. Finally, it can be shown that the combination of spatial derivatives $\odot$ is the one of lowest order that will give the above invariances of δ_1 [6].

For an array of stripes, δ_1 will vanish only if the characteristic wavelength of the stripes is λ everywhere. An array of stripes whose wave vector is $\mathbf{k_1} = k_1 \hat{\mathbf{k}}$ will have a disorder per unit area given by $\bar{\delta}_1 = |k_1^2 - k_0^2|/2$. Thus, in calculating the disorder parameter from (say) experimental data, the best possible value of k_0 should be used [8] (even though the direction of $\mathbf{k}$ can be arbitrary).

As an example, we calculate δ_1 for a "target" pattern (Fig. 2) whose envelope function is

$$A_t(\mathbf{x}) = a e^{i(k_0 r - \mathbf{k}\cdot\mathbf{x})}. \tag{6}$$

Hence $\odot A_t(\mathbf{x}) = k_0 A_t(\mathbf{x})/2r$ [9]. Thus for a target centered in a circle of radius R the disorder parameter is given by

$$\delta_1(\text{target}) = \pi R/k_0\,, \tag{7}$$

while for a target centered in a square domain of side L, $\delta_1 = (L/k_0) \int_0^1 dt\, \sinh^{-1}(t^{-1}) = 1.7627(L/k_0)$. Observe that even though $|\odot A|$ diverges at the origin, each circular shell makes the same contribution to δ_1. This is

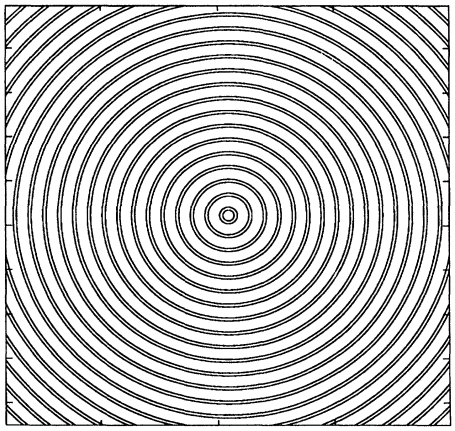

FIG. 2. The "target" pattern given by $U_t(\mathbf{x}) = ae^{ik_0 r}$.

invaluable for the analysis of experimental data, which is typically given on a finite lattice and is noisy. Since $A(\mathbf{x})$ changes rapidly close to a defect, the numerical derivatives evaluated from its values on the lattice are likely to have large errors. Hence the ability to discard data close to a defect is crucial for the analysis of experimental data. The numerical techniques presented below have been checked by evaluating δ_1 from a numerically generated target pattern of ~5 circles with 10% white noise at each lattice point. We find that with ~20 data points per wavelength δ_1 can be estimated to within 3% of the theoretical value.

The extraction of the envelope function from the experimental data is a nontrivial task. If the stripes were pointing in one direction everywhere in space, it would be possible to extract $A(\mathbf{x})$ using spectral methods [10]. The presence of experimental noise, defects, and unknown boundary conditions prevents such an analysis for the patterns shown in Fig. 1. The method described below is numerically inefficient, but works sufficiently accurately. It may be possible to use methods based on wavelet transforms to determine the envelope function more efficiently [11].

We first need to evaluate the analytic signal $A(\mathbf{x}_0)e^{i\psi(\mathbf{x}_0)}$ of the data $U(\mathbf{x})$ in a neighborhood of $\mathbf{x}_0$. This is achieved by fitting data inside a square to the functional form $a(\mathbf{x}_0)\cos[\mathbf{k}(\mathbf{x}_0)\cdot\mathbf{x} + \phi(\mathbf{x}_0)]$. For the cases we studied, square regions centered at $\mathbf{x}_0$ with sizes about the wavelength λ of the stripes give accurate estimates of the parameters [12]. The least squares fitting is done using the Lavenberg-Marquardt method [13,14]. Observe that we not only estimate the parameters but also effectively reduce the noise through the least squares fitting. The parameter estimation is carried out at each point of the lattice, and the wave vector $\mathbf{k}(\mathbf{x}_0)$ is chosen to be as close as possible to the direction of its neighbors. [Thus at certain points we need to choose the direction $-\mathbf{k}(\mathbf{x}_0)$ rather than $\mathbf{k}(\mathbf{x}_0)$. If this were not done the imaginary part of the analytic signal of $U(\mathbf{x})$ would fail to be smooth.] k_0, estimated by averaging the values of $|\mathbf{k}(\mathbf{x}_0)|$ over the entire pattern, agrees with the value estimated from a spectral analysis.

The next task is to obtain the envelope function for the pattern using Eq. (1) for a fixed $\mathbf{k}$, from the analytic signal $a(\mathbf{x})e^{i[\mathbf{k}(\mathbf{x})\cdot\mathbf{x}+\phi(\mathbf{x})]}$. In principle all we need to do is to divide the analytic signal by $e^{i\mathbf{k}\cdot\mathbf{x}}$ to obtain the envelope function $A(\mathbf{x})$. However, one precaution needs to be taken. Since we need to take spatial derivatives of the field, $A(\mathbf{x})$ needs to vary sufficiently slowly on the scale of the lattice. If $\mathbf{k}$ were pointing in the x direction, and $\mathbf{k}(\mathbf{x})$ were pointing close to the negative x direction, we would need many lattice points per wavelength to get reasonably accurate results. We find (by numerical experiments) that with ~20 lattice points per wavelength, the following recipe gives acceptable results. If $\mathbf{k}(\mathbf{x})$ is pointing to the right side of the y axis [i.e., the x component of $\mathbf{k}(\mathbf{x})$ is positive], we choose the direction of $\mathbf{k}$ to be the x direction; if $\mathbf{k}(\mathbf{x})$ is pointing to the left side of the y axis, $\mathbf{k}$ is chosen to be the $-x$ direction.

We have thus partitioned our pattern in two, the analytic signal being expanded as $e^{\pm i\mathbf{k}\cdot\mathbf{x}}$ in the separate domains. In calculating the disorder parameter, we only use those points all of whose nearest neighbors belong to the same partition as the point itself; thus we can use Eq. (2) for the separate domains. We are unable to use the contributions from the center of a defect, or from points on a domain wall pointing along the y direction. But, as we have already indicated, the contributions from these points can be dropped in evaluating the disorder parameter without significant error. Furthermore, since the field $U(\mathbf{x})$ and hence $A(\mathbf{x})$ change rapidly at such points, their contributions are not likely to be accurate.

Figure 3 shows the values of $\bar{\delta}_1$ for 30 patterns generated in the chemical system (five of which are shown in Fig. 1), suggesting two additional significant results. First, observe that the values of $\bar{\delta}_1$ at a given set of parameters are bunched together. Thus not only is $\bar{\delta}_1$ invariant under Euclidean motions of a given pattern, it appears to be a (statistical) invariant of different patterns generated by the system at the same set of control parameters. In addition, the disorder parameter undergoes a sharp increase near the point where the time dependence sets in (when the malonic acid concentration falls below 10.5 mM [2]). Thus, it is possible to identify the onset of pattern dynamics from a purely static measure. Other static measures (such as correlation length) change smoothly though the transition [2].

Irregularities such as targets, dislocations, and domain walls make different contributions to δ_1. Their effects can be differentiated by generalizing δ_1 to a function δ_μ given by taking moments of $|\odot A(\mathbf{x})|$. Specifically, for $\mu < 2$, we define the *generalized disorder* by

$$\delta_\mu = \frac{2-\mu}{k_0^{2\mu}\langle|A(\mathbf{x})|\rangle^\mu}\int\int |\odot A(\mathbf{x})|^\mu \, dx\, dy\,. \qquad (8)$$

The powers of k_0 and $\langle|A|\rangle$ are chosen so that mean disorder $\bar{\delta}_\mu \equiv \delta_\mu / \int\int dx\, dy$ is dimensionless. The condition

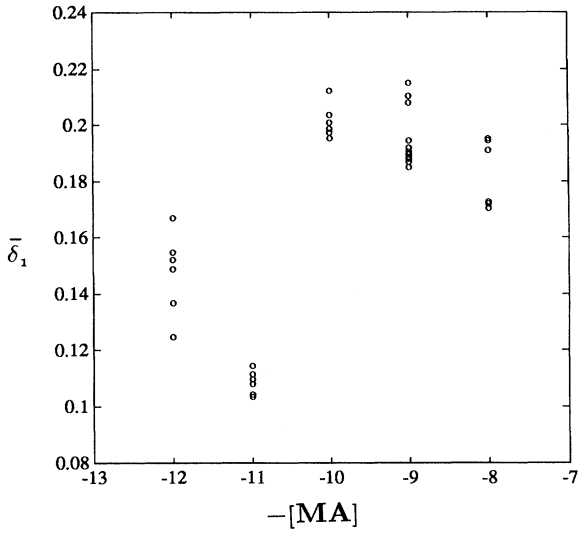

FIG. 3. The values of $\bar{\delta}_1$ as a function of control parameter (negative of malonic acid concentration). The patterns are stationary for the two control parameters on the left, and time dependent for the three on the right. Observe that the values of $\bar{\delta}_1$ for distinct patterns at the same parameters are closely bunched. Notice also that $\bar{\delta}_1$ undergoes a discontinuity near the onset of time dependence in the patterns.

$\mu < 2$ is required to prevent the divergence of the integral at the center of a target. For a target centered in a circle of radius R, $\lim_{\mu\to 2} \delta_\mu = \pi/2k_0^2$. For a domain wall the integral of Eq. (8) is finite, and thus $\lim_{\mu\to 2} \delta_\mu = 0$. Hence $\lim_{\mu\to 2} \delta_\mu$ is proportional to the number of targets in a pattern. Analysis of experimental data is in progress.

Unlike dynamical measures of disorder such as dimension density [15] and Karhunen-Loève decomposition [16], δ_1 is a measure of disorder of a given pattern. The use of the underlying "perfect" structure in its definition provides δ_1 with more information than measures such as correlation length. For example, the disorder parameter for a domain wall between stripes oriented in different directions increases monotonically with the angle between these stripes. The observed sharp increase in δ_1 at the onset of pattern dynamics needs to be studied in numerical as well as other experimental systems.

We have benefited from discussions with M. Golubitsky, M. Gorman, L. Kadanoff, A. Lee, and M. Marder. The computations presented were done on a KSR1 supercomputer at the Texas Center for Advanced Molecular Design. This work is partially funded by the Office of Naval Research (G. H. G. and R. E. J.) and the Department of Energy Office of Basic Energy Sciences (Q. O. and H. L. S.).

*Electronic address: gemunu@uh.edu
†Electronic address: jones@uhphys.phys.uh.edu
‡Electronic address: qi@chaos.ph.utexas.edu
§Electronic address: swinney@chaos.ph.utexas.edu

[1] B. B. Mandelbrot, *Fractal Geometry of Nature* (Freeman, San Francisco, 1982); H. G. E. Hentschel and I. Procaccia, Physica (Amsterdam) **8D**, 435 (1983); T. C. Halsey, M. H. Jensen, L. P. Kadanoff, I. Procaccia, and B. Shraiman, Phys. Rev. A **33**, 1141 (1986); *Time Series Prediction,* edited by A. S. Weigend and N. A. Gershenfeld (Addison-Wesley, Reading, MA, 1994).

[2] Q. Ouyang and H. L. Swinney, Chaos **1**, 411 (1991).

[3] Q. Ouyang and H. L. Swinney, in *Chemical Waves and Patterns,* edited by R. Kapral and K. Showalter (Kluwer, Dordrecht, 1995), pp. 269–295.

[4] Q. Ouyang and H. L. Swinney, Nature (London) **352**, 610 (1991).

[5] A. C. Newell and J. A. Whitehead, J. Fluid Mech. **38**, 279 (1969); L. A. Segel, J. Fluid Mech. **38**, 203 (1969).

[6] G. H. Gunaratne, Phys. Rev. Lett. **71**, 1367 (1993); G. H. Gunaratne, Q. Ouyang, and H. L. Swinney, Phys. Rev. E **50**, 2802 (1994).

[7] To estimate the amount of disorder in a hexagonal pattern, the field $U(\mathbf{x})$ has to be expanded in three basis directions with three envelope functions $A_1(\mathbf{x})$, $A_2(\mathbf{x})$, and $A_3(\mathbf{x})$ [see Eq. (1)]. The disorder parameter for the pattern is obtained by replacing $|\odot A(\mathbf{x})|$ in Eq. (2) by the sum of $|\odot_n A_n(\mathbf{x})|$, where $\odot_n$ (for $n = 1, 2, 3$) has a definition analogous to Eq. (3).

[8] It may be difficult to determine the value of k_0 of the system from experimentally generated pattern; e.g., close to the Eckhaus instability the system is strained away from k_0. If the pattern forming system can be modeled, a linear stability analysis will give k_0.

[9] Thus $|\odot A|$ is proportional to the curvature of the contour lines at any point of the pattern.

[10] S. Rasenat, V. Steinberg, and I. Rehberg, Phys. Rev. A **42**, 5998 (1990); S. Ciliberto, P. Coullet, J. Lega, E. Pampaloni, and C. Perez-Garcia, Phys. Rev. Lett. **65**, 2370 (1990).

[11] T. Passot and A. C. Newell, Physica (Amsterdam) **74D**, 301 (1994); Ph. Tchamitchian and B. Torrésani, in *Wavelets and their Applications,* edited by M. B. Ruskai (Jones and Bartlett Publishers, Boston, 1992), pp. 123–151.

[12] We evaluated k_0 and δ_1 for several sizes of the square used for the least squares fitting. k_0 is independent of the square size, while δ_1 either reaches a limit or passes through a minimum. This stationary value agrees with the analytical result, when the latter can be calculated.

[13] W. H. Press, B. P. Flannery, S. A. Teukolsky, and W. T. Vettering, *Numerical Recipes—The Art of Scientific Computing* (Cambridge University Press, Cambridge, England, 1988).

[14] We assign higher weights to the points closer to the center of the square. The results are independent of the form of the weighting.

[15] D. A. Egolf and H. S. Greenside, Phys. Rev. Lett. **74**, 1751 (1995).

[16] J. D. Rodrigues and L. Sirovich, Physica (Amsterdam) **43D**, 77 (1990); N. Aubry, R. Guyomet, and R. Lima, J. Nonlinear Sci. **2**, 183 (1992).

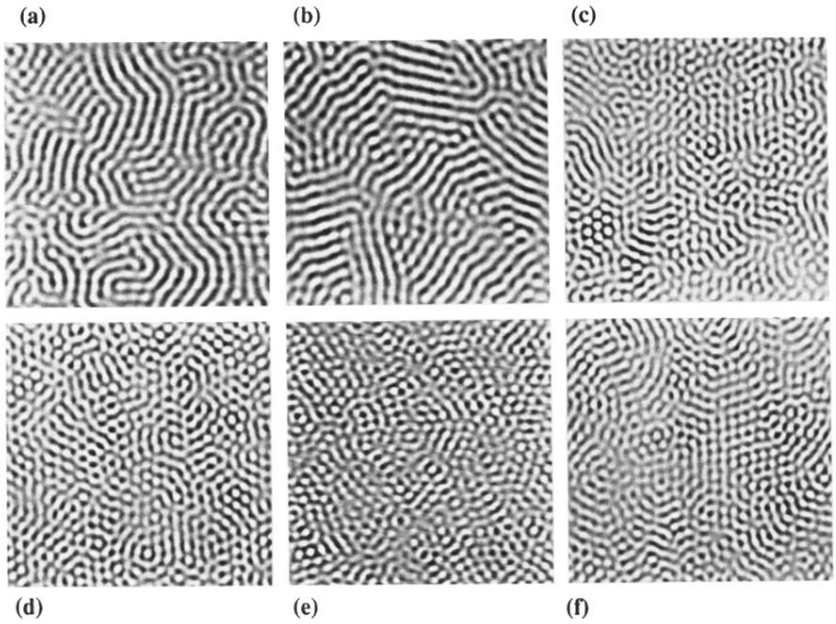

FIG. 1. Patterns generated in a reaction-diffusion system involving a chlorite-iodide-malonic acid reaction in a thin disk reactor. The reaction occurs in a thin layer of polyacrylamide gel sandwiched between two reservoirs, A and B. The malonic acid concentrations in reservoir B were (a) 12.0, (b) 11.0, (c) 10.0, (d) 9.0, (e) 8.0, and (f) 7.0 mM; the malonic acid concentration in reservoir A was 0. Other control parameters were held fixed at $[I^-]_0^{A,B} = 3.0$ mM, $[Na_2SO_4]_0^{A,B} = 4.5$ mM, $[ClO_2{}^-]_0^A = 18$ mM, $[ClO_2{}^-]_0^B = 0$ mM, $[H_2SO_4]_0^A = 0.5$ mM, $[H_2SO_4]_0^B = 20$ mM, temperature 7.0 °C, and gel thickness 2.0 mm. The transition from stationary to time-dependent patterns occurs at a concentration 10.5 mM of malonic acid in reservoir B.